

**POTENTIALS AND LIMITS OF BOSE-EINSTEIN  
INTERFEROMETRY**

**Boris Tomášik<sup>1</sup>**

*Institut für Theoretische Physik, Universität Regensburg, D-93040 Regensburg,  
Germany*

**Ulrich Heinz<sup>2</sup>**

*CERN, Theory Division, CH-1211 Geneva 23, Switzerland  
and Institut für Theoretische Physik, Universität Regensburg, D-93040 Regensburg,  
Germany*

We complete the introduction of Yano-Koonin-Podgoretskiĭ (YKP) parametrization of the correlation function by deriving the corrections to the correlation radii which arise from releasing the popular smoothness approximation and approximation of setting the pair momentum on-shell. We investigate the definition range of this parametrization and find kinematic regions in which the YKP parametrization is inapplicable. These problems disappear if the newly proposed Modified Yano-Koonin-Podgoretskiĭ parametrization is used. We then focus on the physical interpretation of the correlation radii obtained in the different parametrizations. While the extraction of the longitudinal source expansion from the YK rapidity is found to be rather robust against variations of the source density profiles, the extracted emission duration is quite sensitive to such variations and cannot be reliably extracted except for the case of extremely long source lifetimes.

*Dedicated to Ján Pišút  
on occasion of his 60th birthday.*

## 1 Introduction

In recent years Bose-Einstein interferometry [1, 2] for ultrarelativistic heavy ion collisions has been developed into a powerful analysis tool [3, 4]. It turned out that not only the sizes of boson emitting sources are measurable via the magnitude of the so-called *correlation radii*, which are the parameters of a Gaussian fit to the observed correlation function, but also the *source dynamics* leaves its fingerprint in their *dependence on the average momentum of the pair* [5, 6, 7, 8, 9]. On the other hand it became also

---

<sup>1</sup>E-mail address: Boris.Tomasik@physik.uni-regensburg.de

<sup>2</sup>E-mail address: Ulrich.Heinz@cern.ch

clear that the temporal and spatial size parameters of the emitter are not all separately accessible; only certain combinations of the space-time variances of the source are measurable [10, 11, 12]. This knowledge is crucial for an understanding of the usefulness of various Gaussian parametrizations of the correlator. By an appropriate choice of the parametrization one can ensure that the resulting width parameters reflect specific combinations of the space-time variances which allow for a particularly straightforward physical interpretation in terms of specific source features.

It has recently been argued that for sources with dominant longitudinal expansion the *Yano-Koonin-Podgoretskiĭ (YKP) parametrization* of the correlator [13, 14, 15] provides a more direct interpretation of the measurement than the “traditional” *Cartesian* one [14, 10, 11]. It was stated that the YKP parametrization allows for direct observation of the longitudinal expansion of the source and provides a more accurate measurement of the emission duration. These arguments were supported by a study involving a model which was believed to reproduce the data and to include all relevant features admitted by experimental observations [12, 16]. Of course, strictly speaking the “amount” of information gained from a measurement is independent of the chosen parametrization of the correlator (as long as it is complete); the extraction of certain quantities of interest appears, however, easier when using the YKP one. The mathematical equivalence of the different parametrizations leads, on the other hand, to relations between their respective correlation radii which must be satisfied if the analysis was done correctly. The corresponding relations between the Cartesian and YKP radius parameters were given in [12, 16].

In this paper we complete the program of introducing the YKP parametrization. Corrections to the correlation radii due to the off-shellness of the pair momentum  $K$  and due to the so-called smoothness approximation are given up to  $\mathcal{O}(q^2)$ . (The corresponding corrections for the Cartesian parametrization were derived in [17].) Moreover, we study the definition range of this parametrization. We find that kinematic regions can exist where it is not defined. A small modification in the formulation of YKP parametrization is shown to avoid these problems. The cost for this remedy is a slightly less straightforward interpretation of the resulting radius parameters.

With these improved results at hand we can once more study the question of the interpretation of the measured correlation radii in the different parametrizations. We focus in particular on the extraction of the source lifetime (i.e. the emission duration). We find that that the original optimistic statements in this context [12, 16] require qualification – the lifetime measurement turns out to be considerably more model-dependent than originally anticipated. We illustrate this with some simple examples in Section 3.

More technical items are deferred into the appendices. In Appendix A the definition range of YKP parametrization is studied. Relations between the correlation radii of different parametrizations used in this paper are given in Appendix B. Finally, the mentioned  $\mathcal{O}(q^2)$  corrections to the YKP radius parameters are derived in Appendix C.

## 2 Measuring the source

Given the emission function  $S(x, K)$  (Wigner phase-space density of the source) and assuming completely chaotic (independent) production of the particles [23], the correlation function can be calculated via [18, 19, 20, 21, 22]

$$C(q, K) = 1 + \frac{|\int d^4x e^{iq \cdot x} S(x, K)|^2}{\int d^4x S(x, K + \frac{q}{2}) \int d^4y S(y, K - \frac{q}{2})}. \quad (1)$$

Here  $K$  and  $q$  are the average and relative 4-momentum of the particle pair:

$$K = \frac{1}{2}(p_1 + p_2), \quad q = p_1 - p_2. \quad (2)$$

Equation (1) requires the knowledge of the full quantum mechanical structure of the source: the momentum  $K$  in the numerator is off-shell. In practice, however, when evaluating the correlations it is put to its on-shell value by setting

$$K^0 \rightarrow E_K = \sqrt{\mathbf{K}^2 + m^2}. \quad (3)$$

The formalism also simplifies considerably if both momenta in the denominator of (1) are identified with  $K$  (the so-called smoothness approximation). The applied simplifications are expected not to be too serious because the interesting region of correlations lies at small values of  $q$  where the above approximations are good. Nevertheless, corrections due to the above simplifications can be (and will be) derived, which support these superficial statements in a more rigorous way.

To summarize, the above two approximations lead to the relation

$$C(q, K) \approx 1 + \frac{|\int d^4x e^{iq \cdot x} S(x, K)|^2}{|\int d^4x S(x, K)|^2}, \quad (4)$$

with  $K$  taken on-shell according to (3).

It is convenient to parameterize the correlation function in Gaussian form:

$$C(q, K) - 1 = \exp(-q_\mu q_\nu B^{\mu\nu}(K)). \quad (5)$$

Expressions for the elements of the (symmetric) matrix  $B$  are obtained by expanding both (4) and (5) up to second order in  $q$  and identifying the coefficients of both series. This leads to

$$B_{\mu\nu} = \langle \tilde{x}_\mu \tilde{x}_\nu \rangle, \quad (6)$$

where

$$\tilde{x}_\mu = x_\mu - \langle x_\mu \rangle, \quad (7)$$

and  $\langle \dots \rangle$  denotes the average weighted by the emission function:

$$\langle f(x) \rangle(K) = \frac{\int d^4x f(x) S(x, K)}{\int d^4x S(x, K)}. \quad (8)$$

One must, however, keep in mind that correlations of two *physical* particles are measured and therefore  $q$  and  $K$  fulfill the on-shell constraint

$$q \cdot K = 0, \quad (9)$$

which reduces the number of independent  $q$ -components to three. Due to this only certain combinations of the  $B_{\mu\nu}$ 's are experimentally accessible.

In what follows we focus entirely on a class of azimuthally symmetric sources representing the fireballs generated in central collisions. It is common to orient the coordinate system in such a way that the  $z$ -axis (longitudinal,  $l$ ) lies in beam direction and the  $x$ -axis (outward,  $o$ ) in the direction of the transverse component of the pair momentum. The remaining  $y$ -direction is then denoted as sideward ( $s$ ). For azimuthally symmetric sources there exists then a symmetry under the transformation  $y \rightarrow -y$ , leading to only seven non-zero components of  $B$  of which only four combinations are measurable [15]. (Note that no such symmetry is present in the outward direction as long as the directions parallel and antiparallel to  $K_\perp$  are not equivalent.)

In this coordinate frame  $q_s$  decouples from the equation (9). When employing this relation in different ways one arrives at different Gaussian parametrizations of the correlator.

## 2.1 Cartesian parametrization

Resolving the on-shell constraint (9) as

$$q_t = \beta_\perp q_o + \beta_l q_l, \quad (10)$$

where  $\beta_i = K^i/E_K$  and  $q_t$  is the zeroth component of relative momentum, and inserting (10) in (5) leads to the Cartesian parametrization of the correlator [14, 10, 11]

$$C(q, K) - 1 = \exp[-q_s^2 R_s^2(K) - q_o^2 R_o^2(K) - q_l^2 R_l^2(K) - 2q_o q_l R_{ol}^2(K)]. \quad (11)$$

For the correlation radii one obtains

$$R_o^2 = \langle (\tilde{x} - \beta_\perp \tilde{t})^2 \rangle, \quad (12a)$$

$$R_s^2 = \langle \tilde{y}^2 \rangle, \quad (12b)$$

$$R_l^2 = \langle (\tilde{z} - \beta_l \tilde{t})^2 \rangle, \quad (12c)$$

$$R_{ol}^2 = \langle (\tilde{x} - \beta_\perp \tilde{t})(\tilde{z} - \beta_l \tilde{t}) \rangle. \quad (12d)$$

Due to the on-shell constraint (10) spatial and temporal source sizes are mixed in all observable radius parameters except for  $R_s^2$ . This makes the interpretation of a measurement rather involved since the spatial and temporal contributions cannot be resolved in a model-independent manner. The situation simplifies for the longitudinal radius  $R_l^2$  if the frame in which analysis is performed is boosted longitudinally such that  $K_l = \beta_l = 0$  (Longitudinally Co-Moving System, LCMS) [24]. Then

$$R_l^2 = \langle \tilde{z}^2 \rangle, \quad (13c)$$

$$R_{ol}^2 = \langle (\tilde{x} - \beta_\perp \tilde{t}) \tilde{z} \rangle. \quad (13d)$$

So the longitudinal dimension, in the longitudinal rest frame of the pion pair, is measured directly. The cross-term  $R_{o_l}^2$  may obviously take both positive and negative values. The superscript should not confuse – it just expresses the bilinear character (and the dimensionality) of this parameter.

Access to the lifetime is provided by the difference [24]

$$R_{\text{diff}}^2 = R_o^2 - R_s^2 = \beta_{\perp}^2 \langle \tilde{t}^2 \rangle - 2\beta_{\perp} \langle \tilde{x}\tilde{t} \rangle + \langle \tilde{x}^2 - \tilde{y}^2 \rangle. \quad (14)$$

Of course, one has to assume that  $R_{\text{diff}}^2$  is dominated by the first term on the r.h.s., at least at higher  $K_{\perp}$  where the suppression by  $\beta_{\perp}$  is small. In Section 3 we investigate this assumption in more detail.

Note finally that corrections to the correlation radii given by (12) due to the approximation (4) were derived in [17] – they are listed in Appendix C.

## 2.2 Yano-Koonin-Podgoretskiĭ parametrization

When one wants to measure the source using Bose-Einstein interferometry the problem of the “right” frame for the measurement arises. The appropriate choice of frame may even depend on the pair momentum. Only a part of the whole (expanding) fireball size is reflected in the correlation radii, namely that part contributing to production of particles of a given momentum [5]. In the following this particular part of the source will be called *effective source*.

Since the measurements are done in order to obtain information on the local phase-space characteristics (density, energy density, temperature etc.) of the emitter one should expect that the appropriate frame for the measurement of the (effective) source sizes is its own rest frame. Unfortunately, this frame cannot be directly determined in the experiment. However, in [14] Podgoretskiĭ showed for non-expanding sources that the cross-term of the correlator parametrization is a direct consequence of measuring out of the source rest frame. The issue becomes a bit more involved when expanding sources are treated, because then expansion is present also in the effective source. However, since the velocity difference between its edges is not very big, one can still (at least intuitively) introduce something like an average or effective source velocity and try to express the cross-term with its help.

This can be to a large part achieved by resolving the on-shell constraint (9) as

$$q_o = \frac{1}{\beta_{\perp}} q_t - \frac{\beta_l}{\beta_{\perp}} q_l. \quad (15)$$

and rewriting (5) in the so-called *Yano-Koonin-Podgoretskiĭ (YKP) form* [15, 12]:

$$C(q, K) - 1 = \exp[-q_{\perp}^2 R_{\perp}^2(K) - (q_l^2 - q_t^2) R_{\parallel}^2(K) - (R_o^2(K) + R_{\parallel}^2(K))(q \cdot U(K))^2]. \quad (16)$$

Here the three correlation radii are manifestly invariant under longitudinal boosts, and the cross-term has been absorbed into a term involving the Yano-Koonin (YK) velocity  $v_{\text{YK}}$  which is the longitudinal component of the 4-velocity  $U$ :

$$U = \gamma(1, 0, 0, v_{\text{YK}}), \quad \gamma = \frac{1}{\sqrt{1 - v_{\text{YK}}^2}}. \quad (17)$$

Note also that in the Yano-Koonin-Podgoretskiĭ parametrization the components of the transverse momentum difference occur only in the combination

$$q_{\perp} = \sqrt{q_s^2 + q_o^2}. \quad (18)$$

For the YKP correlation radii and the YK velocity one can infer expressions similar to (12) [12, 16]:

$$R_0^2 = A - v_{\text{YK}} C, \quad (19a)$$

$$R_{\perp}^2 = \langle \tilde{y}^2 \rangle = R_s^2, \quad (19b)$$

$$R_{\parallel}^2 = B - v_{\text{YK}} C, \quad (19c)$$

$$v_{\text{YK}} = \frac{A+B}{2C} \left( 1 - \sqrt{1 - \left( \frac{2C}{A+B} \right)^2} \right). \quad (19d)$$

Here we introduced the shorthands

$$A = \langle \tilde{t}^2 \rangle - \frac{2}{\beta_{\perp}} \langle \tilde{x}\tilde{t} \rangle + \frac{1}{\beta_{\perp}^2} \langle \tilde{x}^2 - \tilde{y}^2 \rangle, \quad (20a)$$

$$B = \langle \tilde{z}^2 \rangle - 2 \frac{\beta_l}{\beta_{\perp}} \langle \tilde{x}\tilde{z} \rangle + \frac{\beta_l^2}{\beta_{\perp}^2} \langle \tilde{x}^2 - \tilde{y}^2 \rangle, \quad (20b)$$

$$C = \langle \tilde{t}\tilde{z} \rangle - \frac{1}{\beta_{\perp}} \langle \tilde{x}\tilde{z} \rangle - \frac{\beta_l}{\beta_{\perp}} \langle \tilde{x}\tilde{t} \rangle + \frac{\beta_l}{\beta_{\perp}^2} \langle \tilde{x}^2 - \tilde{y}^2 \rangle. \quad (20c)$$

Note that these shorthands would appear as parameters of a (pseudo-) Cartesian parametrization with the same  $q$ -components as used in YKP [9].

Although the YKP radii are invariant under longitudinal boosts, their interpretation is connected with the frame where  $v_{\text{YK}} = 0$ , the so-called Yano-Koonin frame. In this frame  $C$  vanishes. From (19a) and (20a) one concludes that  $R_0^2$  (and only this parameter) is sensitive to the lifetime  $\langle \tilde{t}^2 \rangle$  of the source in this frame. This has led to some optimism in Refs. [12, 16] because measuring the lifetime in this way seems to be much easier than via  $R_{\text{diff}}^2$  (cf. eq. (14)), due to the missing factor  $\beta_{\perp}^2$  which may be small. (Note that in the YK frame  $R_{\text{diff}}^2 = \beta_{\perp}^2 A$ .) However, as already mentioned in the discussion below (14), both extraction procedures strongly rely on the assumption that the last two terms in (20a) are small. For small  $K_{\perp}$  this is not so clear, due to the small factors  $\beta_{\perp}$  in the denominator: for example, although at  $K_{\perp} = 0$  we generally expect  $\langle \tilde{x}^2 - \tilde{y}^2 \rangle$  to vanish due to azimuthal symmetry, if divided by  $\beta_{\perp}^2$  the limit for  $K_{\perp} \rightarrow 0$  can be a not-zero quantity [16]. The true behaviour of  $A$  for small but nonzero  $K_{\perp}$  can thus only be clarified by model studies. For large  $K_{\perp}$ , on the other hand, different models give different predictions for  $\langle \tilde{x}^2 - \tilde{y}^2 \rangle$  (see next Section). Unless  $\langle \tilde{t}^2 \rangle$  becomes very large (much larger than the geometric contributions  $\langle \tilde{x}^2 \rangle$ ,  $\langle \tilde{y}^2 \rangle$ ), which may happen during compound nucleus formation at low energies [26] but is unlikely for the rapidly disintegrating sources formed in relativistic heavy ion collisions, the extraction of the lifetime thus appears to be quite model-dependent. This reduces the power of  $R_0^2$  (and  $R_{\text{diff}}^2$  as well) for measuring the emission duration. In fact,  $R_0^2$  may even become negative due to the discussed ‘‘correction term’’ [3].

On first sight, since (20b) has a similar structure as (20a), one might conclude that the same problems must appear when extracting the longitudinal source size from  $R_{\parallel}^2$ . Fortunately, here the situation is better since now the sub-leading terms are multiplied with  $\beta_l$  and  $\beta_t^2$ , respectively. In the YK frame this velocity is usually small (see below). Although this is again a model-dependent statement, it appears to be valid for all models which are in agreement with the data. Thus  $R_{\parallel}^2$  is a good estimator for the longitudinal dimension of the source measured in YK frame.

### 2.3 Modified Yano-Koonin-Podgoretskiĭ parametrization

So far, nothing has been said about the definition range and the resulting applicability of YKP parametrization. Clearly, it is not defined for  $K_{\perp} = \beta_{\perp} = 0$  as the on-shell constraint (15) is singular at this point. However, a more serious problem is that the argument of the square root in (19d) can become negative (see Appendix A). Then the YKP parametrization is *ill-defined* (the YKP parameters become complex and thus unphysical). We hasten to stress that *the applicability region of the YKP parametrization cannot be checked directly by the experiment*. It is therefore strongly recommended to cross-check the correlation radii obtained from a YKP fit via the relations (50)/(51) and/or (48)/(49).

As shown in Appendix A, the failure of the YKP parametrization is due to the use of  $q_{\perp}$  instead of  $q_s$  as an independent variable. In other words, the elimination of  $q_o$  via (15) is not done completely. This leads to the appearance of contributions from  $\langle \tilde{y}^2 \rangle / \beta_{\perp}^2$  in (20). One can, however, eliminate  $q_o$  completely without giving up the longitudinal boost-invariance of the fitted radius parameters by writing the correlator in the form

$$C(q, K) - 1 = \exp[-q_s^2 R_{\perp}^{\prime 2}(K) - (q_t^2 - q_{\parallel}^2) R_{\parallel}^{\prime 2}(K) - (R_0^{\prime 2}(K) + R_{\parallel}^{\prime 2}(K))(q \cdot U'(K))^2], \quad (21)$$

with

$$U' = \gamma'(1, 0, 0, v'_{\text{YK}}), \quad \gamma' = \frac{1}{\sqrt{1 - v_{\text{YK}}^{\prime 2}}}. \quad (22)$$

This will be called the *Modified Yano-Koonin-Podgoretskiĭ* (YKP') parametrization. For its correlation radii one finds

$$R_0^{\prime 2} = A' - v'_{\text{YK}} C', \quad (23a)$$

$$R_{\perp}^{\prime 2} = \langle \tilde{y}^2 \rangle = R_{\perp}^2 = R_s^2, \quad (23b)$$

$$R_{\parallel}^{\prime 2} = B' - v'_{\text{YK}} C', \quad (23c)$$

$$v'_{\text{YK}} = \frac{A' + B'}{2C'} \left( 1 - \sqrt{1 - \left( \frac{2C'}{A' + B'} \right)^2} \right), \quad (23d)$$

where

$$A' = \langle \tilde{t}^2 \rangle - \frac{2}{\beta_{\perp}} \langle \tilde{x} \tilde{t} \rangle + \frac{1}{\beta_{\perp}^2} \langle \tilde{x}^2 \rangle = A + \frac{1}{\beta_{\perp}^2} \langle \tilde{y}^2 \rangle, \quad (24a)$$

$$B' = \langle \tilde{z}^2 \rangle - 2 \frac{\beta_l}{\beta_\perp} \langle \tilde{x}\tilde{z} \rangle + \frac{\beta_l^2}{\beta_\perp^2} \langle \tilde{x}^2 \rangle = B + \frac{\beta_l^2}{\beta_\perp^2} \langle \tilde{y}^2 \rangle, \quad (24b)$$

$$C' = \langle \tilde{t}\tilde{z} \rangle - \frac{1}{\beta_\perp} \langle \tilde{x}\tilde{z} \rangle - \frac{\beta_l}{\beta_\perp} \langle \tilde{x}\tilde{t} \rangle + \frac{\beta_l}{\beta_\perp^2} \langle \tilde{x}^2 \rangle = C + \frac{\beta_l}{\beta_\perp^2} \langle \tilde{y}^2 \rangle. \quad (24c)$$

The interpretation of  $R_0'^2$  and  $R_\parallel'^2$  is again easiest in the frame where  $v'_{\text{YK}} = 0$ , the “Modified Yano-Koonin (YK’) frame”. It is not as straightforward as in case of the original YKP radii. This is the price for a parametrization which is defined everywhere. While in YKP parametrization one could hope that the last “correction terms” of (20a), (20b), and (20c) are small, now only the (large) term  $\langle \tilde{x}^2 \rangle$  appears instead of the (smaller) difference  $\langle \tilde{x}^2 - \tilde{y}^2 \rangle$ . Therefore, the deviations of  $R_0'^2$  and  $R_\parallel'^2$  from  $\langle \tilde{t}^2 \rangle$  and  $\langle \tilde{z}^2 \rangle$ , respectively, are larger than those of  $R_0^2$  and  $R_\parallel^2$ . Still, for the measurement of the longitudinal size  $\langle \tilde{z}^2 \rangle$  the situation may not be bad because  $\langle \tilde{x}^2 \rangle$  in (24b) is again multiplied by  $\beta_l^2$ , which is small in the YK’ frame, exactly like discussed above in case of  $R_\parallel^2$ . A measurement of  $\langle \tilde{t}^2 \rangle$  via  $R_0'^2$ , on the other hand, is definitely impossible.

A good feature which is preserved in the Modified YKP parametrization is that the velocity  $v'_{\text{YK}}$  still maps to a very good approximation the velocity of the effective source. This will be demonstrated in the next Section.

Finally, we note that while the relative momentum components used in the original YKP parametrization satisfy the inequality

$$q_\perp \geq q_o = \frac{1}{\beta_\perp} q_t - \frac{\beta_l}{\beta_\perp} q_l, \quad (25)$$

which means that the data points never fill the whole three-dimensional  $q$ -space, no such restriction exists for  $q_s$  which is used in the modified YKP parametrization. This should help to avoid certain technical problems in the fitting procedure which can occur with the YKP parametrization.

**Cross-relations** Since all parametrizations discussed so far are just different representations of the same correlation function, there must exist relations between their correlation radii. They are listed in Appendix B.

These relations provide a powerful check of the correctness of results obtained from fitting the measured correlation function with Gaussian parametrizations; if Cartesian and YKP (and eventually Modified YKP) fits are performed independently, the resulting correlation radii must fulfill the corresponding cross-check relations. Such control is *strongly recommended in order to avoid the pitfalls related to the possible non-existence of the YKP parametrization* for the data under study (which may not show up clearly in the fitting process but might cause it to converge to a wrong result).

**Off-shell corrections** Before closing this section we study the corrections to the YKP and Modified YKP correlation radii connected with the approximations made in (4). They are easily inferred by combining the known expressions (55) and (56) according to (51) and (53). The resulting corrections are given in Appendix C. In the case of the Modified YKP parametrization an interesting phenomenon is observed:



while the correction terms accounting for the release of the smoothness approximation  $P_1(p_1)P_1(p_2) \approx [P_1(K)]^2$  in the denominator (where  $P_1(p) = \int d^4x S(x, p)$  is the invariant single-particle spectrum) and those accounting for the release of the on-shell approximation  $K^0 \approx E_K$  in the numerator diverge separately in the limit  $K_\perp \rightarrow 0$ , this singularity cancels in their sum. For the YKP parametrization the singularities already cancel at the level of the individual corrections. The reason for this difference is the use of  $q_\perp$  in the YKP parametrization (instead of  $q_s$  as in the modified one), leading to the appearance of  $R_{\text{diff}}^2$  in (51) (instead of  $R_o^2$  in (53)).

### 3 Examples

In this Section we illustrate some statements made in the previous Section with the help of a model for a longitudinally and transversely expanding fireball which is locally thermalized. This is neither an extensive model study nor an analysis of real data. Therefore we will stay on a rather superficial level and won't go very deeply into the model structure.

Our model (in fact it is a class of models) is expressed by the emission function [8, 9, 16]

$$\begin{aligned} S(x, K) d^4x &= \frac{1}{(2\pi)^3} M_\perp \cosh(Y - \eta) \exp\left(-\frac{K \cdot u(x)}{T}\right) \\ &\times G(r) \exp\left(-\frac{(\eta - \eta_0)^2}{2 \Delta\eta^2}\right) \\ &\times \frac{\tau d\tau}{\sqrt{2\pi} \Delta\tau^2} \exp\left(-\frac{(\tau - \tau_0)^2}{2 \Delta\tau^2}\right) d\eta r dr d\varphi. \end{aligned} \quad (26)$$

The momentum is parameterized here in terms of transverse mass  $M_\perp = \sqrt{K_\perp^2 + m^2}$ , rapidity  $Y$ , and the transverse momentum  $K_\perp$  such that

$$K = (M_\perp \cosh Y, K_\perp, 0, M_\perp \sinh Y). \quad (27)$$

As space-time coordinates in the transverse plane we use the usual polar coordinates  $r$  and  $\varphi$ , and the remaining two directions are parameterized by longitudinal proper time  $\tau = \sqrt{t^2 - z^2}$  and space-time rapidity  $\eta = 0.5 \ln[(t + z)/(t - z)]$ . The  $\eta$ -profile is chosen to be Gaussian with width  $\Delta\eta$  and the center at  $\eta_0$ . The freeze-out times are distributed by a Gaussian of width  $\Delta\tau$  centered around the average freeze-out time  $\tau_0$ .

We will study models with two different transverse profiles: a *Gaussian* one

$$G(r) = \exp\left(-\frac{r^2}{2 R_G^2}\right), \quad (28)$$

and a *box-shaped* one

$$G(r) = \theta(R_B - r). \quad (29)$$

The dynamics of the source is implemented via the velocity field  $u(x)$ ,

$$u(x) = (\cosh \eta_t \cosh \eta, \cos \varphi \sinh \eta_t, \sin \varphi \sinh \eta_t, \cosh \eta_t \sinh \eta), \quad (30)$$

**Table 1** Values of model parameters used in the calculation

	box	Gauss
temperature $T$	0.1 GeV	
transverse flow scaling parameter $\eta_f$	0.57	0.64
geometric transverse radius $R_B/R_G$	13 fm	6.5 fm
average freeze-out proper time $\tau_0$	7.5 fm/c	
mean proper emission duration $\Delta\tau$	2 fm/c	
width of the space-time rapidity profile $\Delta\eta$	1.3	
pion mass	0.139 GeV/c <sup>2</sup>	
kaon mass	0.493 GeV/c <sup>2</sup>	

where the transverse expansion rapidity  $\eta_t$  is assumed to scale linearly with the radial distance  $r$ :

$$\eta_t = \eta_f \frac{r}{r_{\text{rms}}}. \quad (31)$$

$\eta_f$  is the scaling factor. Note that the transverse rms radius for the Gaussian source is

$$r_{\text{rms}} = \sqrt{2}R_G, \quad (32)$$

while for the box-shaped transverse profile (29) one has

$$r_{\text{rms}} = \frac{R_B}{\sqrt{2}}. \quad (33)$$

The same rms radius is thus ensured by setting  $R_B = 2R_G$ . The source dynamics shows up in the coupling of the velocity field (30) with the momentum (27) via the Boltzmann factor  $\exp[-K \cdot u/T]$ ;  $T$  is the freeze-out temperature. Using (27) and (30) the scalar product in the exponent is written as

$$K \cdot u = M_{\perp} \cosh(Y - \eta) \cosh \eta_t - K_{\perp} \cos \varphi \sinh \eta_t. \quad (34)$$

For our calculation we take the data-inspired parameter values listed in Table 1. They are not obtained from a careful fit to the data, but seem to reproduce the measured correlations from Pb+Pb collisions at 160 AGeV/c [27, 28] reasonably well. Note that the different values of  $\eta_f$  used in the two models lead to the *same average transverse expansion velocity*  $\bar{v}_{\perp}$  in both cases. This allows for a better comparison of the results, since  $\bar{v}_{\perp}$  appears to be the relevant (model-independent) physical quantity expressing the strength of the transverse collective expansion. The transverse sizes  $R_G$  and  $R_B$  are chosen such that the resulting rms radii in both models are equal.

In order to provide the reader with a more intuitive picture we show in Fig. 1 transverse cuts of these sources as seen by midrapidity pions of transverse momentum  $K_{\perp} = 0.4$  GeV/c. The different shape of the effective sources obtained from the two models is crucial for an understanding of the  $M_{\perp}$ -dependences of the correlation radii. These will be studied in what follows.

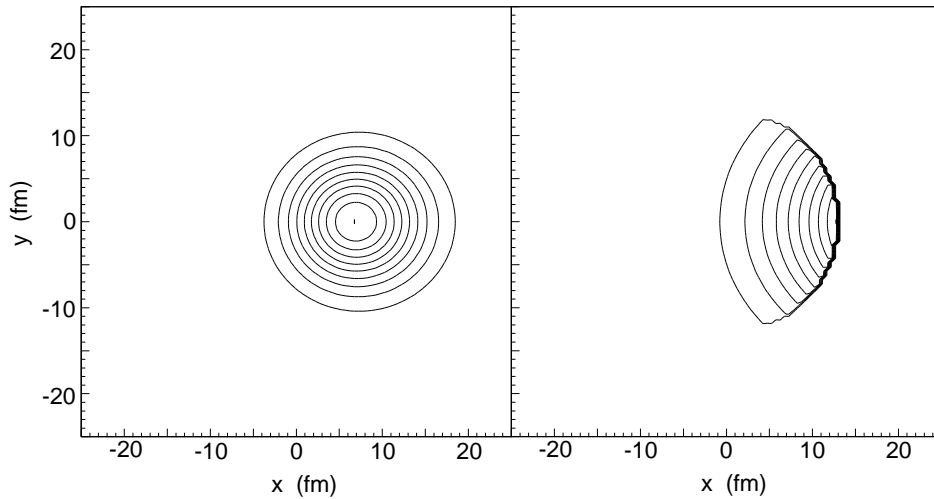


**Figure 1** Transverse cuts of the two models from Table 1 at  $\eta_0 = 0$  for midrapidity pions ( $Y = 0$ ) of transverse momentum  $K_\perp = 0.4 \text{ GeV}/c$ . Left: Gaussian source; right: box-shaped source. (Note that the “corners” of the box-shaped source are a plotting artifact.)

### 3.1 $M_\perp$ -dependence of the correlation radii

In Figs. 2 and 3 we show the  $M_\perp$ -dependences of the correlation radii of all mentioned parametrizations. We evaluate the radii in the LCMS, and in order to get a non-vanishing cross-term and Yano-Koonin velocity we take particles at slightly forward rapidity ( $Y = 0$ ,  $\eta_0 = -1$ ). We compute both pion and kaon correlations. Instead of plotting the Yano-Koonin velocity in Fig. 3c we show the Yano-Koonin rapidity

$$Y_{\text{YK}} = \frac{1}{2} \ln \frac{1 + v_{\text{YK}}}{1 - v_{\text{YK}}}. \quad (35)$$

In Fig. 3c' we show the modified YK rapidity, defined via an analogous relation involving  $v'_{\text{YK}}$ .

Let us comment on a few characteristic features. Although the average transverse expansion velocity is the same in both models, the box-shaped source generates a stronger  $M_\perp$ -dependence of  $R_s$  than the Gaussian one. This effect is even stronger for  $R_o$ . Moreover for higher transverse mass  $R_o$  is smaller than  $R_s$  for the box-shaped source while the opposite is true for the Gaussian source. This results from the different shapes of the effective sources shown in Fig. 1: while for the Gaussian transverse profile the effective source for higher  $M_\perp$  expands into the dilute tail of the density distribution, for the box-profile it is squeezed towards the outer boundary, leading to much smaller widths, especially in the outward direction. Note that this has important phenomenological consequences: even if the temperature is known, the exact amount of transverse flow cannot be inferred uniquely from the shape of  $R_s(M_\perp)$  without making assumptions

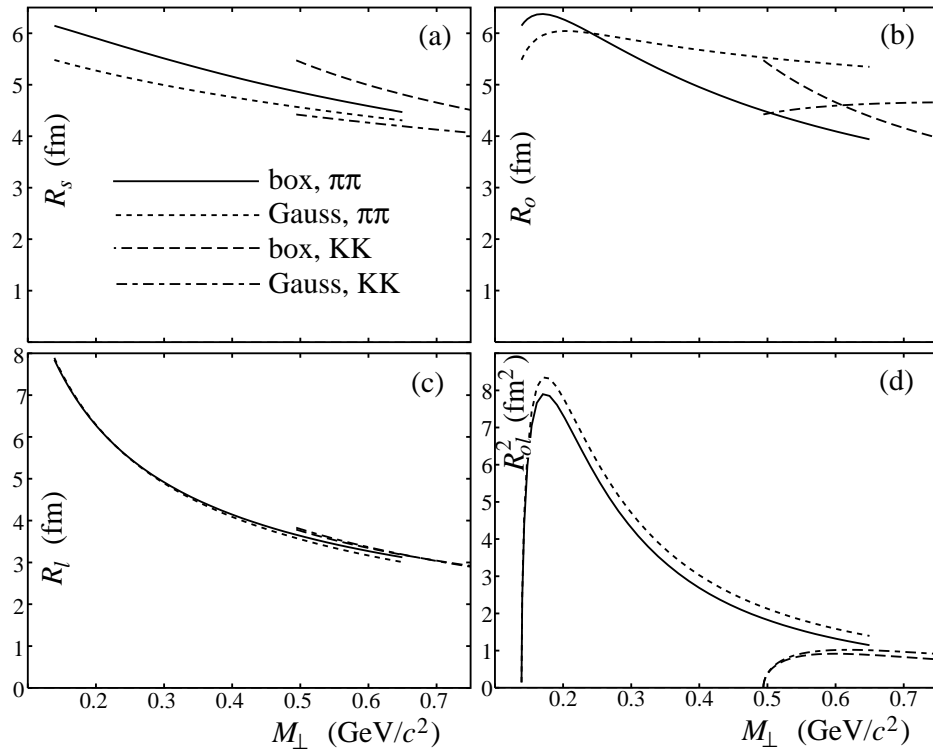


**Figure 2** Correlation radii of the Cartesian parametrization for the models introduced in (26) with parameter values from Table 1. The calculation is performed in the LCMS for particle pairs at slightly forward rapidity ( $\eta_0 = -1$ ). Both pion (solid and dotted lines) and kaon (dashed and dash-dotted lines) correlations were computed. Transverse profiles: box (solid, dashed), Gauss (dotted, dash-dotted).

about the transverse source geometry. By combining measurements of  $R_s$  and  $R_o$ , however, one should be able to shed some light on this question. Definitely, this problem will deserve a more detailed study when fitting real data.

The mentioned behaviour is also reflected in the  $M_\perp$ -dependence of  $R_0^2$ . For a box-shaped source  $\langle \tilde{x}^2 \rangle < \langle \tilde{y}^2 \rangle$ ; via the last term in (20a) this leads to negative values of  $R_0^2$ . For kaons from this source the YKP parametrization does not even exist in the studied kinematic region.

This last problem does not exist in the Modified YKP parametrization, as seen in Fig. 3. The behaviour of  $R_0^2$  is completely dominated by the last term in (24a). The comparison of both models is in accord with Fig. 2.

Since the longitudinal geometry and dynamics are identical in both models, no differences are observed in the behaviour of the longitudinal correlation radii. Even in

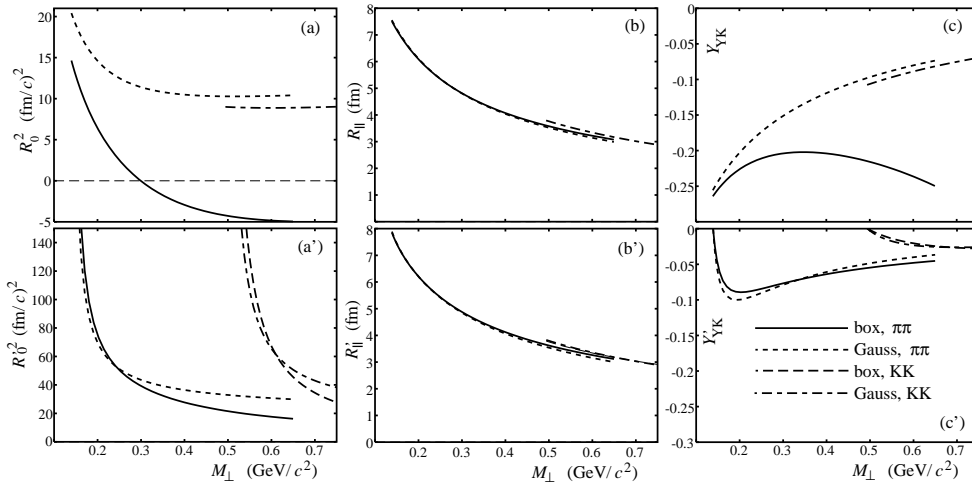


**Figure 3** YKP (upper row) and Modified YKP (lower row) radii for the same models and the same kinematics as in Fig. 2. Note that  $R_{\perp} = R'_{\perp} = R_s$ . Line symbols are as in Fig. 2. At the given kinematics no YKP parametrization exists for kaons from the box-shaped source.

case of  $R_{\parallel}^2$  the correction terms (the last two terms in (24b)) lead to negligible effects, since they are multiplied by  $\beta_t^2$  which is small in the YK frame.

### 3.2 YK rapidity and source velocity

Since the direct access to the effective source velocity is probably the main strength of the YKP/Modified YKP parametrization, Fig. 4 is entirely devoted to the investigation of this particular feature. The velocity parameters are again encoded via the corresponding rapidities as introduced in (35). In Fig. 4a we show the characteristic dependence of the Yano-Koonin rapidity on the pair rapidity for a longitudinally (boost-invariantly) expanding source, as observed in the source center-of-mass (CMS) frame. The modified YK rapidity behaves in the same way. Note that the modified YK rapidity seems to be rather insensitive to the shape of the transverse density profile. This was already seen in Fig. 3c'. Fig. 4b (which is in fact a compilation of Figs. 3c and 3c') shows the  $M_{\perp}$ -dependence of these rapidities for  $Y = 1$  in the CMS.

As discussed in the previous section, it is important to check to what extent the Yano-Koonin velocity really coincides with the velocity of the effective source. We also discussed the ambiguity of defining the latter for expanding effective sources. Here we study the difference  $Y_{\text{diff}}$  between the YK and/or Modified YK rapidity and the space-time rapidity (which is also the longitudinal fluid rapidity) of the point of maximal emissivity  $\eta_{\text{max}}$  (maximum of the emission function). While for most studied cases this difference is positive for  $Y_{\text{YK}} > 0$  and negative in the opposite case (i.e. the YK/Modified YK velocity is “faster” than the fluid velocity at the maximum emissivity point), it is

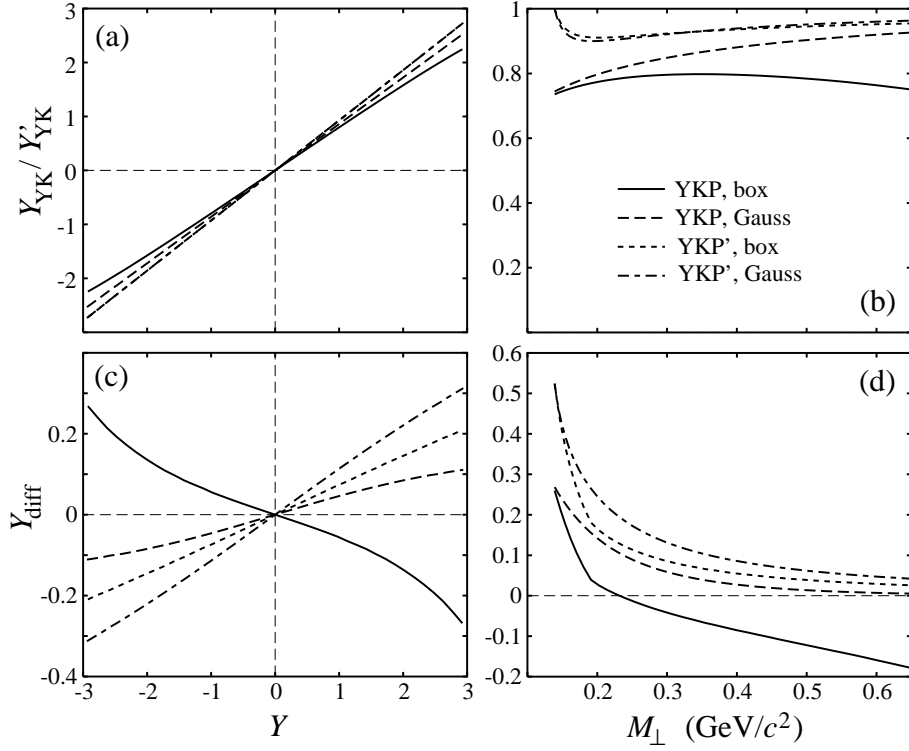


**Figure 4** Investigation of the YK/YK' rapidities resulting from the two studied models: box-shaped (solid and dotted line) and Gaussian (dashed and dash-dotted) (see text). Quantities related to YKP parametrization are plotted by solid and dashed lines, those related to the YKP' one by dotted and dash-dotted lines. (a) YK/YK' rapidity as function of pair rapidity  $Y$  studied in the center-of-mass (CMS) frame of the fireball,  $K_{\perp} = 0.3 \text{ GeV}/c$ , note that dotted and dash-dotted line coincide; (b) the same quantities as functions of  $M_{\perp}$  for  $Y = 1$  calculated in the source CMS ( $\eta_0 = 0$ ); (c) the difference  $Y_{\text{diff}}$  between the YK/YK' rapidity and the space-time rapidity of the point of maximal emissivity (maximum of the emission function) as function of  $Y$ ,  $K_{\perp} = 0.3 \text{ GeV}/c$ ; (d) the same quantity but as function of  $M_{\perp}$  for  $Y = 1$ ,  $\eta_0 = 0$ .

the other way around for high  $M_{\perp}$  pions from the box-shaped source. This difference is therefore again a model-dependent feature. However, it is important to stress that in all cases  $Y_{\text{diff}}$  is considerably smaller than  $Y_{YK}$  or  $Y'_{YK}$ . Note also that, as discussed before, the rapidity  $\eta_{\text{max}}$  may well not be the “right” one to express the rapidity of effective source: if the source expands there is always an ambiguity of how to define its rapidity. Our choice is one of several possibilities. The small value of  $Y_{\text{diff}}$  should thus not be taken quantitatively as the difference between the experimentally accessible quantity  $Y_{YK}$  and the true source rapidity; its smallness rather indicates that the former maps

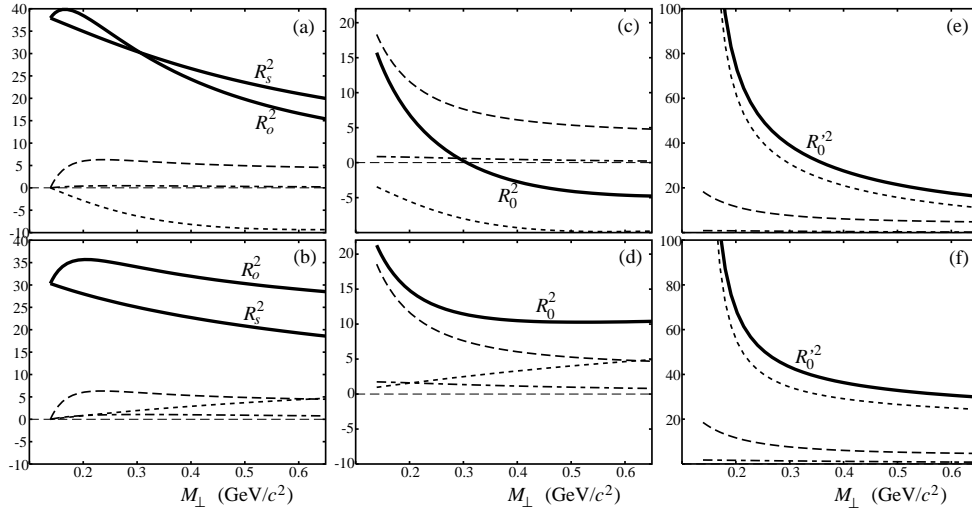


**Figure 5** Correlation radii related to the emission duration (plotted by thick solid lines) as functions of  $M_{\perp}$ . Upper row: box-shaped source, lower row: Gaussian source (see text). The remaining curves show the individual contributions: (a) and (b):  $\beta_{\perp}^2 \langle \tilde{t}^2 \rangle$  (dashed),  $\langle \tilde{x}^2 - \tilde{y}^2 \rangle$  (dotted) and  $-2\beta_{\perp} \langle \tilde{x} \tilde{t} \rangle$  (dash-dotted); (c) and (d): same as before but all terms divided by  $\beta_{\perp}^2$ ; (e) and (f): same as (c) and (d) but the dotted line corresponds to  $\langle \tilde{x}^2 \rangle / \beta_{\perp}^2$ . Units on the ordinate are  $\text{fm}^2$ .

the latter very well. We conclude that the measurement of longitudinal expansion in this way is reliable and does not depend on particular assumptions about the transverse geometry. This is valid for both YKP and YKP' parametrizations.

### 3.3 The emission duration

In order to analyze the measurement of the emission duration in more detail, we show in Fig. 5 the relevant correlation radii of all three parametrizations studied in this paper, together with the individual contributions out of which they are constructed. This study was performed for pions at  $Y = \eta_0 = 0$ ; in this case the LCMS and YK frame coincide and the decomposition is easy. This Figure can be summarized as follows: the geometric contribution  $\langle \tilde{x}^2 - \tilde{y}^2 \rangle$  is at least as important as the temporal contribution  $\langle \tilde{t}^2 \rangle$ . This is even more true for the box-shaped source: here  $R_o^2 < R_s^2$  and  $R_o^2 < 0$ . The reason for this is the rapid decrease of the size in outward direction which was illustrated in Fig. 1. Note that such a behaviour was suggested in [25] as a possible indicator for opacity of the source, i.e., surface-dominated emission. We see here that already a source with a box-shaped transverse density profile exhibits this “opacity signature” for large  $K_{\perp}$ , as clearly seen in Fig. 1. For us, however, it is important to conclude that, unless  $c^2 \langle \tilde{t}^2 \rangle$  is considerably larger than the geometric size of the source, the lifetime cannot be reliably extracted from interferometric measurement as one cannot really

correct for contributions from the transverse geometry. There exist many combinations of  $\langle \tilde{t}^2 \rangle$  and  $\langle \tilde{x}^2 - \tilde{y}^2 \rangle$  which all lead to the same interferometric signal.

We finally note that, as shown in Figs. 5e,f, the radius parameter  $R_0'^2$  in the modified YKP parametrization does not allow for an extraction of the source lifetime, as already anticipated in Section 2.  $R_0'^2$  is seen to be completely dominated by the term  $\langle \tilde{x}^2 \rangle / \beta_\perp^2$  and practically insensitive to  $\langle \tilde{t}^2 \rangle$ .

## 4 Conclusions

We have shown that the recently advocated YKP parametrization is not defined for all choices of kinematic variables. It is important to stress that this non-definiteness can only be identified experimentally through comparison of fit results from different parametrizations via the relations introduced in Appendix B. As it is hard to interpret fit results from a possibly ill-defined parametrization it is absolutely necessary to perform such comparisons and cross-checks, and one should worry seriously about cases where inconsistencies appear!

A Modified YKP parametrization was introduced which does not suffer from these problems. Eventually, it therefore also can serve for the check of the YKP radius parameters extracted from a fit to the data [27]. The corresponding relations were given in Appendix B.

It was shown that the velocity parameters of both YKP and Modified YKP parametrizations accurately reflect the longitudinal velocity of the effective source. This feature appears to be fairly model-independent. The idea [14] of introducing these velocity parameters as the effective velocity of a non-expanding effective source thus remains valid in the context of strongly expanding emitters.

Our consideration of the measurement of the emission duration showed that it is practically impossible to extract this quantity in a model-independent way. On the other hand, clear differences in the correlation patterns resulting from models with Gaussian and with box-shaped transverse profiles were observed. These could help to decide between models which are more or less suitable for a description of the data. In fact, recent studies show that a box-shaped source fits the data of the NA49 collaboration better than a Gaussian one [28]. By making such specific assumptions about the transverse source geometry (and only then) the emission duration can be extracted from the data fit.

**Acknowledgments:** The work of BT was supported by DAAD. The work of UH was supported by DFG, BMBF and GSI. We acknowledge stimulating discussions with Daniel Ferenc and Urs Wiedemann and thank Josef Sollfrank for a careful reading of the manuscript.

Since this is a Festschrift contribution, BT wants to take the opportunity to thank Ján Pišút for the honour to belong to his students and friends. I have learned a lot from him and physics makes much more fun when taught by people like Ján. UH would like to thank Ján for the pleasure of many good scientific exchanges and collaborations, as well as for sending so many good young students to Regensburg for visits which have



always been scientifically very fruitful. We join the other congratulants: all the best, Ján!

### A Definition range for the YKP/Modified YKP parameters

The Yano-Koonin velocity  $v_{\text{YK}}$  is only defined if the discriminant

$$D = (A + B)^2 - 4C^2, \quad (36)$$

is positive. Here we study the conditions for that. From (24) it is clear that

$$A' \geq 0, \quad (37a)$$

$$B' \geq 0, \quad (37b)$$

so we conclude

$$|A' + B'| = A' + B'. \quad (38)$$

It can be proven that

$$D' = (A' + B')^2 - 4C'^2 \geq 0, \quad (39)$$

or

$$|A' + B'| - 2|C'| \geq 0, \quad (40)$$

i.e., the modified Yano-Koonin velocity is defined everywhere. Indeed, due to (38) inequality (40) may be written as

$$A' + B' \mp 2C' \geq 0, \quad (41)$$

where the upper sign stands for  $C' > 0$  and the lower for  $C' < 0$ . Inserting expressions (24) leads to

$$A' + B' \mp 2C' = \left\langle \left\{ \left( \tilde{t} - \frac{1}{\beta_{\perp}} \tilde{x} \right) \mp \left( \tilde{z} - \frac{\beta_l}{\beta_{\perp}} \tilde{x} \right) \right\}^2 \right\rangle \geq 0. \quad (42)$$

This proves (39) – the modified YKP parametrization is defined everywhere (except, of course, the point  $K_{\perp} = \beta_{\perp} = 0$  [12, 16]).

From expressions (24) one also can see that

$$A + B = A' + B' - \frac{1 + \beta_l^2}{\beta_{\perp}^2} \langle \tilde{y}^2 \rangle, \quad (43)$$

$$2C = 2C' - \frac{2\beta_l}{\beta_{\perp}^2} \langle \tilde{y}^2 \rangle. \quad (44)$$

It is therefore possible to obtain negative values for  $D$ :

$$D = (A + B)^2 - 4C^2 < 0. \quad (45)$$

For example, if  $\beta_l = 0$  and  $\langle \tilde{y}^2 \rangle$  has a value bigger than  $\langle \tilde{x}^2 \rangle$ , there exist values for  $\beta_\perp$  such that

$$|A + B| = |A' + B' - \frac{1}{\beta_\perp^2} \langle \tilde{y}^2 \rangle| < 2|C'| = 2|C|. \quad (46)$$

Hence, there are kinematic regions where the YKP parametrization is not defined. (For example see Section 3.)

## B Relations between correlation radii of different parametrizations

In this Appendix relations between correlation radii of various parametrizations are listed.

The simplest and most obvious one is

$$R_s^2 = R_\perp^2 = R'_\perp{}^2. \quad (47)$$

The remaining YKP parameters are related to the modified ones in a simple way:

$$A = \gamma'^2 \left( R_0'^2 + v_{\text{YK}}'^2 R_\parallel'^2 \right) - \frac{1}{\beta_\perp^2} R_\perp'^2, \quad (48a)$$

$$B = \gamma'^2 \left( R_\parallel'^2 + v_{\text{YK}}'^2 R_0'^2 \right) - \frac{\beta_l^2}{\beta_\perp^2} R_\perp'^2, \quad (48b)$$

$$C = \gamma'^2 v_{\text{YK}}' \left( R_0'^2 + R_\parallel'^2 \right) - \frac{\beta_l}{\beta_\perp^2} R_\perp'^2, \quad (48c)$$

and the inverse relations are given by

$$A' = \gamma^2 \left( R_0^2 + v_{\text{YK}}^2 R_\parallel^2 \right) + \frac{1}{\beta_\perp^2} R_\perp^2, \quad (49a)$$

$$B' = \gamma^2 \left( R_\parallel^2 + v_{\text{YK}}^2 R_0^2 \right) + \frac{\beta_l^2}{\beta_\perp^2} R_\perp^2, \quad (49b)$$

$$C' = \gamma^2 v_{\text{YK}} \left( R_0^2 + R_\parallel^2 \right) + \frac{\beta_l}{\beta_\perp^2} R_\perp^2. \quad (49c)$$

Similar relations exist, of course, between the original and/or modified YKP parameters and the Cartesian correlation radii. The latter are expressed in terms of YKP parametrization [12, 16]

$$R_o^2 - R_s^2 \equiv R_{\text{diff}}^2 = \beta_\perp^2 \gamma^2 \left( R_0^2 + v_{\text{YK}}^2 R_\parallel^2 \right), \quad (50a)$$

$$R_l^2 = (1 - \beta_l^2) R_\parallel^2 + \gamma^2 (\beta_l - v_{\text{YK}})^2 \left( R_0^2 + R_\parallel^2 \right), \quad (50b)$$

$$R_{ol}^2 = \beta_\perp \left( -\beta_l R_\parallel^2 + \gamma^2 (\beta_l - v_{\text{YK}}) \left( R_0^2 + R_\parallel^2 \right) \right), \quad (50c)$$

while the inverse relations read

$$A = \frac{1}{\beta_{\perp}^2} R_{\text{diff}}^2, \quad (51a)$$

$$B = R_l^2 - 2\frac{\beta_l}{\beta_{\perp}} R_{ol}^2 + \frac{\beta_l^2}{\beta_{\perp}^2} R_{\text{diff}}^2, \quad (51b)$$

$$C = -\frac{1}{\beta_{\perp}} R_{ol}^2 + \frac{\beta_l}{\beta_{\perp}^2} R_{\text{diff}}^2. \quad (51c)$$

If instead of the original one the Modified YKP parametrization is used then

$$R_o^2 = \beta_{\perp}^2 \gamma'^2 \left( R_0'^2 + v_{\text{YK}}'^2 R_{\parallel}^{\prime 2} \right), \quad (52a)$$

$$R_l^2 = (1 - \beta_l^2) R_{\parallel}^{\prime 2} + \gamma'^2 (\beta_l - v_{\text{YK}}')^2 \left( R_0'^2 + R_{\parallel}^{\prime 2} \right), \quad (52b)$$

$$R_{ol}^2 = \beta_{\perp} \left( -\beta_l R_{\parallel}^{\prime 2} + \gamma'^2 (\beta_l - v_{\text{YK}}') \left( R_0'^2 + R_{\parallel}^{\prime 2} \right) \right), \quad (52c)$$

and

$$A' = \frac{1}{\beta_{\perp}^2} R_o^2, \quad (53a)$$

$$B' = R_l^2 - 2\frac{\beta_l}{\beta_{\perp}} R_{ol}^2 + \frac{\beta_l^2}{\beta_{\perp}^2} R_o^2, \quad (53b)$$

$$C' = -\frac{1}{\beta_{\perp}} R_{ol}^2 + \frac{\beta_l}{\beta_{\perp}^2} R_o^2. \quad (53c)$$

Note that the only formal change in (52)/(53) if compared with (50)/(51) is the replacement of  $R_{\text{diff}}^2$  with  $R_o^2$  and the use of primed radius parameters.

### C Off-shell corrections to the YKP/Modified YKP correlation radii

In this Appendix we list the correction terms to the Gaussian width parameters of the correlator which arise from releasing the approximations made in (4), namely:

(Ad) setting  $P_1(p_1)P_1(p_2) \rightarrow [P_1(K)]^2$  in denominator of that relation – these corrections are denoted with  $\delta_d$ ;

(An) replacing  $K$  with its on-shell value in the emission function appearing in the numerator, i.e.,  $K^0 \rightarrow E_K = \sqrt{\mathbf{K}^2 + m^2}$  – corresponding terms will be assigned with  $\delta_n$ .

Here

$$P_1(p) = \int d^4x S(x, p), \quad (54)$$

denotes the single-particle invariant momentum distribution. In fact, only the correction terms to the shorthands (20) and (24) are derived; those for the YKP/Modified YKP radii can then be obtained via (19)/(23).

The following relations are obtained by combining the correction terms known for the Cartesian parametrization [17]. They read for (Ad)

$$\delta_d R_s^2 = \frac{1}{4K_\perp} \frac{d}{dK_\perp} \ln P_1(K), \quad (55a)$$

$$\delta_d R_o^2 = \frac{1}{4} \frac{d^2}{dK_\perp^2} \ln P_1(K), \quad (55b)$$

$$\delta_d R_l^2 = \frac{1}{4} \frac{d^2}{dK_l^2} \ln P_1(K), \quad (55c)$$

$$\delta_d R_{ol}^2 = \frac{1}{4} \frac{d^2}{dK_\perp dK_l} \ln P_1(K), \quad (55d)$$

and for (An)

$$\delta_n R_s^2 = -\frac{1}{2} \frac{d}{dm^2} \ln P_1(K), \quad (56a)$$

$$\delta_n R_o^2 = -\frac{1}{2} (1 - \beta_\perp^2) \frac{d}{dm^2} \ln P_1(K), \quad (56b)$$

$$\delta_n R_l^2 = -\frac{1}{2} (1 - \beta_l^2) \frac{d}{dm^2} \ln P_1(K), \quad (56c)$$

$$\delta_n R_{ol}^2 = \frac{1}{2} \beta_\perp \beta_l \frac{d}{dm^2} \ln P_1(K). \quad (56d)$$

Now we have to combine these terms according to (51) and (53). The most trivial correction, of course, is the one belonging to  $R_\perp^2$  and  $R_\perp'^2$  as these radius parameters are identical with  $R_s^2$ :

$$\delta_d R_\perp^2 = \delta_d R_\perp'^2 = \delta_d R_s^2 = \frac{1}{4K_\perp} \frac{d}{dK_\perp} \ln P_1(K). \quad (57)$$

For the remaining parameters one finds

$$\delta_d A = \frac{1}{4\beta_\perp^2} \left( \frac{d^2}{dK_\perp^2} - \frac{1}{K_\perp} \frac{d}{dK_\perp} \right) \ln P_1(K), \quad (58a)$$

$$\delta_d B = \frac{1}{4} \left[ \widehat{\mathcal{D}}^2 - \frac{\beta_l^2}{\beta_\perp^2} \frac{1}{K_\perp} \frac{d}{dK_\perp} \right] \ln P_1(K), \quad (58b)$$

$$\delta_d C = -\frac{1}{4} \left[ \widehat{\mathcal{D}} + \frac{\beta_l}{\beta_\perp} \frac{1}{K_\perp} \right] \frac{d}{dK_\perp} \ln P_1(K), \quad (58c)$$

where two operators have formally been introduced

$$\widehat{\mathcal{D}} = \frac{d}{dK_l} - \frac{\beta_l}{\beta_\perp} \frac{d}{dK_\perp}, \quad (59a)$$

$$\widehat{\mathcal{D}}^2 = \frac{d^2}{dK_l^2} - \frac{2\beta_l}{\beta_\perp} \frac{d^2}{dK_l dK_\perp} + \frac{\beta_l^2}{\beta_\perp^2} \frac{d^2}{dK_\perp^2}. \quad (59b)$$

Corresponding relations for the modified radii read

$$\delta_d A' = \frac{1}{4\beta_\perp^2} \frac{d^2}{dK_\perp^2} \ln P_1(K), \quad (60a)$$

$$\delta_d B' = \frac{1}{4} \widehat{\mathcal{D}}^2 \ln P_1(K), \quad (60b)$$

$$\delta_d C' = -\frac{1}{4} \frac{1}{\beta_\perp} \widehat{\mathcal{D}} \frac{d}{dK_\perp} \ln P_1(K). \quad (60c)$$

On the first sight, these correction terms diverge as  $\beta_\perp \rightarrow 0$ . In fact, such a divergence cannot be *a priori* excluded in (20)/(24). One might argue that  $\langle \tilde{x}^2 - \tilde{y}^2 \rangle$ ,  $\langle \tilde{t}\tilde{x} \rangle$ , and  $\langle \tilde{z}\tilde{x} \rangle$  in (20) should vanish for  $\beta_\perp \rightarrow 0$  due to restored azimuthal symmetry; it is, however, not guaranteed that they vanish sufficiently fast. Fortunately, the apparent singularities actually cancel: rewriting  $M_\perp = \sqrt{K_\perp^2 + m^2}$

$$\frac{d}{dK_\perp} = \frac{K_\perp}{M_\perp} \frac{d}{dM_\perp}, \quad (61a)$$

$$\frac{d^2}{dK_\perp^2} = \frac{m^2}{M_\perp^3} \frac{d}{dM_\perp} + \frac{K_\perp^2}{M_\perp^2} \frac{d^2}{dM_\perp^2}, \quad (61b)$$

we find

$$\delta_d A = \frac{E_K^2}{4M_\perp^2} \left[ \frac{d^2}{dM_\perp^2} - \frac{1}{M_\perp} \frac{d}{dM_\perp} \right] \ln P_1(K), \quad (62a)$$

$$\delta_d B = \frac{1}{4} \left[ \widehat{\mathcal{D}}'^2 - \frac{\beta_l E_K^2}{M_\perp^3} \frac{d}{dM_\perp} \right] \ln P_1(K), \quad (62b)$$

$$\delta_d C = -\frac{1}{4} \frac{E_K}{M_\perp} \left[ \widehat{\mathcal{D}}' + \frac{\beta_l E_K}{M_\perp^2} \right] \frac{d}{dM_\perp} \ln P_1(K), \quad (62c)$$

and

$$\delta_d A' = \frac{E_K^2}{4M_\perp^2} \left[ \frac{d^2}{dM_\perp^2} + \frac{1}{\beta_\perp^2} \frac{m^2}{E_K^2 M_\perp} \frac{d}{dM_\perp} \right] \ln P_1(K), \quad (63a)$$

$$\delta_d B' = \frac{1}{4} \left[ \widehat{\mathcal{D}}'^2 + \frac{\beta_l^2}{\beta_\perp^2} \frac{m^2}{M_\perp^3} \frac{d}{dM_\perp} \right] \ln P_1(K), \quad (63b)$$

$$\delta_d C' = -\frac{1}{4} \frac{E_K}{M_\perp} \left[ \widehat{\mathcal{D}}' - \frac{\beta_l}{\beta_\perp^2} \frac{m^2}{E_K M_\perp^2} \frac{d}{dM_\perp} \right] \ln P_1(K), \quad (63c)$$

with

$$\widehat{\mathcal{D}}' = \frac{d}{dK_l} - \frac{\beta_l E_K}{M_\perp} \frac{d}{dM_\perp}, \quad (64a)$$

$$\widehat{\mathcal{D}}'^2 = \frac{d^2}{dK_l^2} - \frac{2\beta_l E_K}{M_\perp} \frac{d^2}{dK_l dM_\perp} + \frac{\beta_l^2 E_K^2}{M_\perp^2} \frac{d^2}{dM_\perp^2}. \quad (64b)$$

From (62) one sees that the correction terms belonging to the YKP parametrization behave well. The singularities cancel thanks to the appearance of  $R_{\text{diff}}^2$  in (51). In

case of the modified parametrization  $R_o^2$  appears instead of  $R_{\text{diff}}^2$  in (53), and thus the correction terms (63) still diverge for vanishing  $\beta_\perp$ .

Corrections due to approximation (An) are obtained in a similar way as above. The one corresponding to  $R_\perp^2$  (and  $R_\perp'^2$  as well) is again obvious

$$\delta_n R_\perp^2 = \delta_n R_\perp'^2 = \delta_n R_s^2 = -\frac{1}{2} \frac{d}{dm^2} \ln P_1(K), \quad (65)$$

and the relations for YKP parametrization are

$$\delta_n A = \frac{1}{2} \frac{d}{dm^2} \ln P_1(K), \quad (66a)$$

$$\delta_n B = -\frac{1}{2} \frac{d}{dm^2} \ln P_1(K), \quad (66b)$$

$$\delta_n C = 0. \quad (66c)$$

For the modified YKP parameters one finds

$$\delta_n A' = \frac{1}{2} \frac{\beta_\perp^2 - 1}{\beta_\perp^2} \frac{d}{dm^2} \ln P_1(K), \quad (67a)$$

$$\delta_n B' = -\frac{1}{2} \left(1 + \frac{\beta_l^2}{\beta_\perp^2}\right) \frac{d}{dm^2} \ln P_1(K), \quad (67b)$$

$$\delta_n C' = -\frac{1}{2} \frac{\beta_l}{\beta_\perp^2} \frac{d}{dm^2} \ln P_1(K). \quad (67c)$$

While the corrections to the YKP parameters are clearly regular, this is not true for the modified ones. These may be rewritten by using

$$\frac{d}{dm^2} = \frac{1}{2} \frac{1}{M_\perp} \frac{d}{dM_\perp}. \quad (68)$$

This leads to

$$\delta_n A' = \frac{1}{4} \frac{1}{M_\perp} \frac{\beta_\perp^2 - 1}{\beta_\perp^2} \frac{d}{dM_\perp} \ln P_1(K), \quad (69a)$$

$$\delta_n B' = -\frac{1}{4} \left(1 + \frac{\beta_l^2}{\beta_\perp^2}\right) \frac{1}{M_\perp} \frac{d}{dM_\perp} \ln P_1(K), \quad (69b)$$

$$\delta_n C' = -\frac{1}{4} \frac{\beta_l}{\beta_\perp^2} \frac{1}{M_\perp} \frac{d}{dM_\perp} \ln P_1(K). \quad (69c)$$

If now these corrections are added to those due to (Ad) displayed in (63), one finally arrives at the total correction terms to the modified YKP radii:

$$\delta A' = \frac{1}{4} \frac{1}{M_\perp} \left[ \frac{E_K^2}{M_\perp} \frac{d^2}{dM_\perp^2} + \left(1 - \frac{E_K^2}{M_\perp^2}\right) \frac{d}{dM_\perp} \right] \ln P_1(K), \quad (70a)$$

$$\delta B' = \frac{1}{4} \left[ \widehat{\mathcal{D}}'^2 - \frac{1}{M_\perp} \left(1 + \frac{\beta_l^2 E_K^2}{M_\perp^2}\right) \frac{d}{dM_\perp} \right] \ln P_1(K), \quad (70b)$$

$$\delta C' = -\frac{1}{4} \frac{E_K}{M_\perp} \left[ \widehat{\mathcal{D}}' + \frac{\beta_l E_K}{M_\perp^2} \right] \frac{d}{dM_\perp} \ln P_1(K). \quad (70c)$$

Note that no divergences survive in the final expressions.

### References

- [1] M. Gyulassy, S.K. Kauffmann, L.W. Wilson: *Phys. Rev. C* **20** (1979), 2267;
- [2] D.H. Boal, C.K. Gelbke, B.K. Jennings: *Rev. Mod. Phys.* **62** (1990), 553;
- [3] U. Heinz: in *Proceedings of 2nd Catania Relativistic Ion Studies CRIS '98*, (S. Costa et al. eds.), World Scientific, 1998, (nucl-th/9806512).
- [4] U. Heinz: in *Correlation and Clustering Phenomena in Subatomic Physics*, (M.N. Harakeh, O. Scholten, J.H. Koch eds.), NATO ASI Series B, Plenum, New York, 1997, (nucl-th/9609029).
- [5] A.N. Makhlin, Yu.M. Sinyukov: *Z. Phys. C* **39** (1988), 69;
- [6] S.V. Akkelin, Yu.M. Sinyukov: *Z. Phys. C* **72** (1996), 501;
- [7] U.A. Wiedemann, P. Scotto, U. Heinz: *Phys. Rev. C* **53** (1996), 918;
- [8] T. Csörgő, B. Lörstad: *Phys. Rev. C* **54** (1996), 1390;
- [9] B. Tomášik, U. Heinz: *Eur. Phys. J. C* **4** (1998), 327;
- [10] M. Herrmann, G.F. Bersch: *Phys. Rev. C* **51** (1995), 328;
- [11] S. Chapman, P. Scotto, U. Heinz: *Phys. Rev. Lett.* **74** (1995), 4400;
- [12] U. Heinz et al.: *Phys. Lett. B* **382** (1996), 181;
- [13] F.B. Yano, S.E. Koonin: *Phys. Lett. B* **78** (1978), 556;
- [14] M.I. Podgoretskiĭ: *Sov. J. Nucl. Phys.* **37** (1983), 272;
- [15] S. Chapman, J.R. Nix, U. Heinz: *Phys. Rev. C* **52** (1995), 2694;
- [16] Y.-F. Wu et al.: *Eur. Phys. J. C* **1** (1998), 599;
- [17] S. Chapman, P. Scotto, U. Heinz: *Heavy Ion Physics* **1** (1995), 1;
- [18] E.V. Shuryak: *Phys. Lett. B* **44** (1973), 387;
- [19] E.V. Shuryak: *Sov. J. Nucl. Phys.* **18** (1974), 667;
- [20] S. Pratt: *Phys. Rev. Lett.* **53** (1984), 1219;
- [21] S. Pratt, T. Csörgő, J. Zimányi: *Phys. Rev. C* **42** (1990), 2646;
- [22] S. Chapman, U. Heinz: *Phys. Lett. B* **340** (1994), 250;
- [23] G.F. Bertsch, P. Danielewicz, M. Herrmann: *Phys. Rev. C* **49** (1994), 442;
- [24] T. Csörgő, S. Pratt: in *Proc. of the Workshop on Relativistic Heavy Ion Physics*, preprint KFKI-1991-28/A, p.75.
- [25] H. Heiselberg, A.P. Vischer: *Eur. Phys. J. C* **1** (1998), 593;
- [26] M.A. Lisa et al.: *Phys. Rev. Lett.* **71** (1993), 2863; and: *Phys. Rev. C* **49** (1994), 2788;
- [27] H. Appelshäuser et al. (NA49 collaboration): *Eur. Phys. J. C* **2** (1998), 661;
- [28] B. Tomášik: *Dissertation*, Universität Regensburg, in preparation.